coatings

MDPI

Article

Flexural Strength and Vickers Microhardness of Graphene-Doped SnO_2 Thin-Film-Coated Polymethylmethacrylate after Thermocycling

Canan Akay [1,2], Gülce Çakmak [3], Mustafa Borga Donmez [3,4,*], Samir Abou-Ayash [3], Emre Mumcu [1,5], Suat Pat [2,5,6] and Burak Yilmaz [3,7,8]

1 Department of Prosthodontics, Faculty of Dentistry, University of Eskisehir Osmangazi, Eskisehir 26040, Turkey; cnngcr2@hotmail.com (C.A.); emremum@yahoo.com (E.M.)
2 Translational Medicine Research and Clinical Center, Eskisehir Osmangazi University, Eskisehir 26040, Turkey; suatpat26@hotmail.com
3 Department of Reconstructive Dentistry and Gerodontology, School of Dental Medicine, University of Bern, 3012 Bern, Switzerland; guelce.cakmak@unibe.ch (G.Ç.); samir.abou-ayash@unibe.ch (S.A.-A.); burak.yilmaz@unibe.ch (B.Y.)
4 Department of Prosthodontics, Faculty of Dentistry, Istinye University, Istanbul 34010, Turkey
5 Advanced Material Technologies Application and Research Center, Eskisehir Osmangazi University, Eskisehir 26040, Turkey
6 Department of Physics, University of Eskisehir Osmangazi, Eskisehir 26040, Turkey
7 Department of Restorative, Preventive and Pediatric Dentistry, School of Dental Medicine, University of Bern, 3012 Bern, Switzerland
8 Division of Restorative and Prosthetic Dentistry, The Ohio State University, Columbus, OH 43210, USA
* Correspondence: mustafa-borga.doenmez@unibe.ch

Abstract: Removable dental prostheses are commonly fabricated using polymethylmethacrylate, a material that does not have favorable mechanical properties and needs reinforcement with particles such as graphene. The aim of this study was to evaluate the flexural strength (FS) and Vickers microhardness of a heat-polymerized polymethylmethacrylate coated with graphene-doped stannic oxide (SnO_2) thin films using a thermionic vacuum arc method after thermocycling. Forty bar-shaped specimens (65 × 10 × 3 mm) were fabricated using a heat-polymerized denture base resin and divided into four groups according to the graphene-doped SnO_2 thin film surface coating performed: No-coat (uncoated), Coat-15 s (coating duration of 15 s), Coat-20 s (coating duration of 20 s), and Coat-30 s (coating duration of 30 s) (n = 10). The thermionic vacuum arc method was used to coat both surfaces of the specimens of each test group with varying durations, and surface coating was verified using Fourier Transform Infrared Spectroscopy. Specimens were subjected to 10,000 cycles of thermocycling. Atomic force microscopy was used to evaluate the surfaces of all specimens before and after thermocycling. Microhardness values were measured five times and averaged. Then, each specimen was subjected to a three-point bending test, and FS values were calculated. Data were analyzed using one-way analysis of variance and Bonferroni tests (α = 0.05). Differences among test groups were nonsignificant when FS data were considered (p = 0.605). However, significant differences were observed among test groups when Vickers microhardness data were considered ($p < 0.001$). Coat-30 s had the highest hardness ($p \leq 0.003$), while the difference among remaining groups were nonsignificant ($p \geq 0.166$). Graphene-doped SnO_2 thin film surface coatings did not significantly affect the FS of tested heat-polymerized denture base resin but increased the Vickers microhardness when the coating duration was 30 s.

Keywords: graphene; flexural strength; microhardness; thermionic vacuum

Citation: Akay, C.; Çakmak, G.; Donmez, M.B.; Abou-Ayash, S.; Mumcu, E.; Pat, S.; Yilmaz, B. Flexural Strength and Vickers Microhardness of Graphene-Doped SnO_2 Thin-Film-Coated Polymethylmethacrylate after Thermocycling. *Coatings* **2023**, *13*, 1106. https://doi.org/10.3390/coatings13061106

Academic Editor: Marek Szindler

Received: 23 May 2023
Revised: 9 June 2023
Accepted: 13 June 2023
Published: 16 June 2023

1. Introduction

Polymethylmethacrylate (PMMA) has been the preferred material for the fabrication of complete dentures [1,2] due to its biocompatibility, low cost, polishability, and ease of

processing and repair [3–6]. However, PMMA has low flexural strength (FS), hardness, toughness, and elastic modulus [7]. Thus, PMMA is susceptible to fracture [8], which can compromise its clinical success [9]. Advancements in computer-aided design and computer-aided manufacturing (CAD-CAM) technologies have facilitated the fabrication of denture bases as an alternative to conventional heat-polymerized PMMA [3]. Subtractively manufactured, prepolymerized PMMA disks were shown to have higher mechanical properties compared with conventional heat-polymerized PMMA considering their standardized and controlled polymerization, performed under high temperature and pressure [4,5]. However, the implementation of CAD-CAM technologies might not be suitable for every clinician or dental technician considering the costs related to milling units, auxiliary equipment, CAD-CAM disks, and maintenance.

Enhancing the mechanical properties of denture base resins has become a subject of interest over the years [7], and various methods for their improvement have been suggested [8]. However, developments in nanotechnology have enabled the use of nano-sized particles, tubes, and fibers as reinforcement phases for denture base materials [10,11]. Graphene, which is a crystalline form of carbon [12] and has an arrangement in a honeycomb pattern [13] that increases its surface area [1], has been incorporated as a reinforcement phase in polymers, including PMMA [14]. A recent study has also concluded that graphene-reinforced, prepolymerized PMMA had higher FS and microhardness than prepolymerized PMMA before and after thermocycling [15].

The thermionic vacuum arc (TVA) method is a physical vapor deposition technique that has a reduced carbon footprint, requires no precursor or buffer gases such as argon [16], and has been used for homogenous thin film deposition [17]. This method allows the deposition of materials in solid, liquid, and gas form [18]. A recent study introduced TVA for the production of graphene-doped stannous (SnO) and stannic oxide (SnO_2) thin films [19]. SnO_2 is an antibacterial material [20,21] that has high stability, high oxidation potential, and corrosion resistance [22–24]. Thus, coating PMMA surfaces with graphene-doped SnO_2 may combine the advantages of graphene and SnO_2, decreasing the possibility of infections in the long-term and improving the mechanical properties of the material, such as surface hardness. Previous studies evaluating the effect of graphene on the properties of denture base resins investigated either prepolymerized graphene-reinforced denture base resins [12–15] or conventional denture base resins enriched with graphene nanoparticles [25–27]. However, to the authors' knowledge, the effect of graphene-doped SnO_2 coatings on the mechanical properties of denture base resins has not been investigated yet. Therefore, the purpose of the present study was to evaluate the effect of graphene-doped SnO_2 (SnO_2-graphene) thin film coatings on the flexural strength (FS) and Vickers hardness of a heat-polymerized denture base resin depending on the duration of the TVA process. The first hypothesis was that the duration of the TVA process would affect the FS, and the second hypothesis was that that the duration of the TVA process would affect the Vickers microhardness of heat-polymerized denture base resin after thermocycling.

2. Materials and Methods

2.1. Specimen Preparation

A total of 40 bar-shaped specimens (65 × 10 × 3 mm) were fabricated using a heat-polymerized denture base resin (High Quality Heat Cure Denture Base Acrylic Resin; PYRAX, Roorkee, India). Specimens were polished with grit silicon carbide abrasive papers (#800-#4000, 3M ESPE, St Paul, MN, USA) under running water using a polishing machine (Gripo 2V; Metkon, Bursa, Turkey). All specimens were then ultrasonically cleaned in distilled water for 15 min and air dried. Digital calipers (Absolute Digimatic; Mitutoyo, Tokyo, Japan) were used to measure the dimensions to ensure a uniform final thickness. Specimens were randomly divided into 4 groups using the randomization function of a software (Excel; Microsoft, Seattle, WA, USA) according to surface coating procedure (n = 10). The number of specimens in each group was determined based on a power analysis with effect size f = 0.42, a = 0.05, and $1 - \beta = 0.8$.

2.2. TVA Application

The TVA system consisted of a short -distance electron gun, which is a 10-mm long Wehnelt cylinder with a tungsten filament that acts as the cathode and a tungsten evaporation crucible, which is the anode. Graphene flakes were mixed with SnO_2 powder with a ratio of 5% to 95% and pressed into pellets prior to deposition, which prevented flakes from being vacuumed during the TVA process. These pellets were placed onto the anode crucible. After the inner pressure of the vacuum chamber reached to 9×10^{-5} torr, an alternating current with a magnitude of 20 A was applied to the tungsten filament of the cathode. This current led to the emission of electrons from the filament, which were attracted by the direct current of 600 V applied to the anode. These electrons heated the pellets and increased their evaporation rate. Combined with the increasing inner chamber pressure, the evaporated material converted to plasma, which deposited onto the specimen placed in the chamber (Figure 1). Simultaneously, the applied voltage was dropped to 0 V and the discharge currents was increased to 0.6 A. The duration of the TVA process was an adjustable parameter, and its value was adjusted to 15, 20, and 30 s. The duration of the TVA process is critical, as longer durations may convert graphene into graphite [28]. Both sides of the samples were coated, and the thickness of the coating was approximately 20 nm given the short duration of the TVA process. The control group (No-coat) was left uncoated.

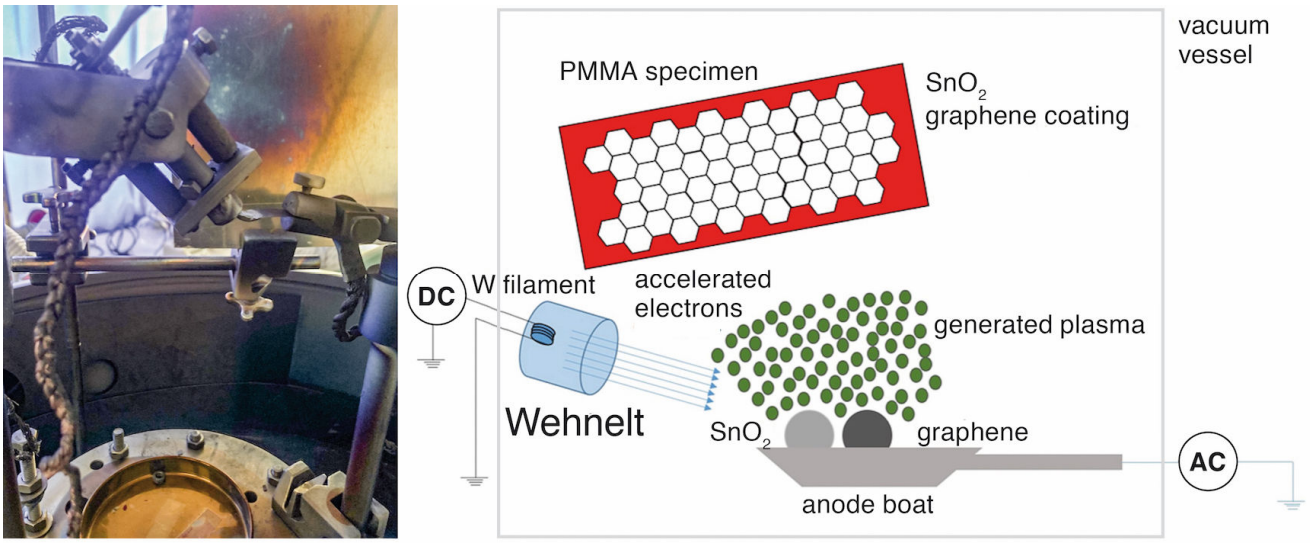

Figure 1. Thermionic vacuum arc system and its schematic design.

Surface coating of the TVA-treated groups were evaluated using Fourier Transform Infrared Spectroscopy (FTIR) and Raman spectroscopy. For FTIR analysis, a total of 32 scans at 4 cm^{-1} were obtained from each specimen between 400 and 4000 cm^{-1}, and all measurements were recorded in attenuated total reflectance mode. All groups other than no-coat had a perceivable peak at 3400.18 cm^{-1}, which corresponded to the FTIR spectra and confirmed graphene deposition on specimen surfaces (Figure 2). Graphene peaks at room temperature were evaluated using a Raman microscope (inVia Raman microscope; Renishaw, Gloucestershire, UK) with a 735-nm laser. Atomic force microscopy (AFM, Q-Scope 400; Ambios Technology, Santa Cruz, CA, USA) was used to evaluate the surface topography of all groups. The gold-doped silicon cantilever of the AFM had a radius smaller than 35 nm, and all images were taken at room temperature. Scanning frequency was adjusted to 3 Hz and cantilever frequency was adjusted to 190 kHz. Specimens were then subjected to 10,000 thermal cycles (SD Mechatronic Thermocycler; SD Mechatronic GmbH, Feldkirchen-Westerham, Germany) at 5–55 °C with a dwell time of 30 s and a transfer time of 10 s [13,29]. After thermocycling, AFM evaluations were repeated. Field emission scanning electron microscopy (FESEM) images of one specimen from each group

were also taken at 10 kV and ×10,000 magnification before and after thermocycling for surface characterization (Regulus 8230; Hitachi, Tokyo, Japan).

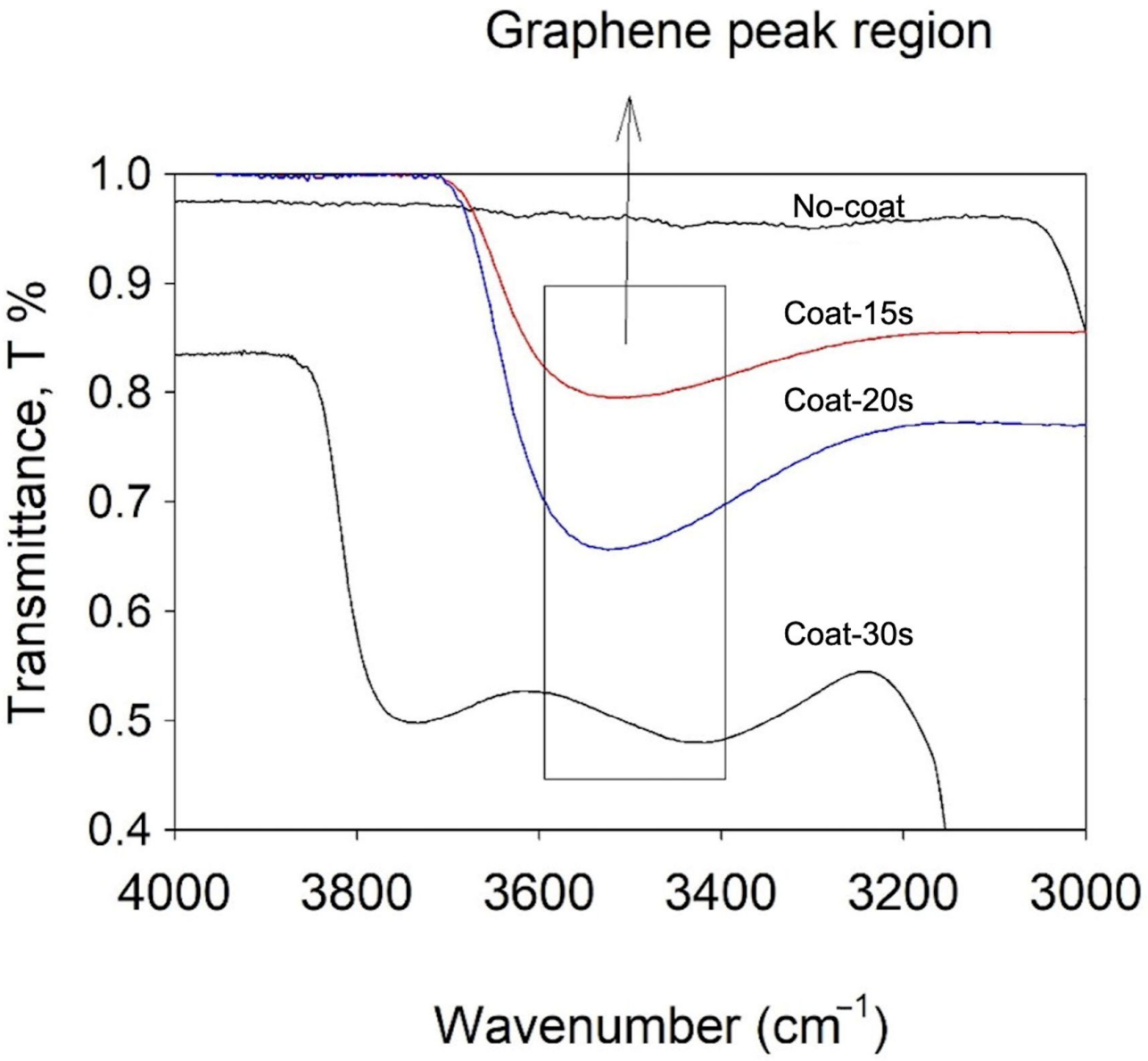

Figure 2. Fourier Infrared Transform Spectroscopy analysis of graphene-coated groups (blue arrow indicates transmittance peak of graphene).

2.3. Microhardness and 3-Point Flexural Strength Tests

Microhardness values of the specimens were measured 5 times, which were then averaged, by applying 25 gf for 30 s with a Vickers hardness tester (Fischerscope HM2000; Helmut-Fischer, Sindelfingen, Germany) [15]. For the 3-point bending test, the samples were placed horizontally on 2 stainless-steel supports that were 50 mm apart. The load was applied to the midpoint of the sample using a 5 kN load cell with a blunt-round end tip (Ø 2 mm) at a crosshead speed of 5 mm/min using a universal testing machine (Instron; Instron Corp, Canton, MA, USA) [30]. The maximum load at fracture was noted and FS of each specimen was calculated. Figure 3 illustrates the 3-point bending test and the formula used for calculations [8]. High-energy coatings, such as TVA, are based on ion implantation that leads to the doping of materials that are nano-level thin. Thus, this layer is not treated as a secondary material during the 3-point bending test, which is performed on a macro level, and the equation was taken from classical mechanics of materials to

test the flexural strength of specimens with rectangular cross-sections. Nevertheless, the thickness of SnO_2-graphene-coated groups were measured prior to 3-point bending test using the same digital caliper to ensure standardized thickness among groups.

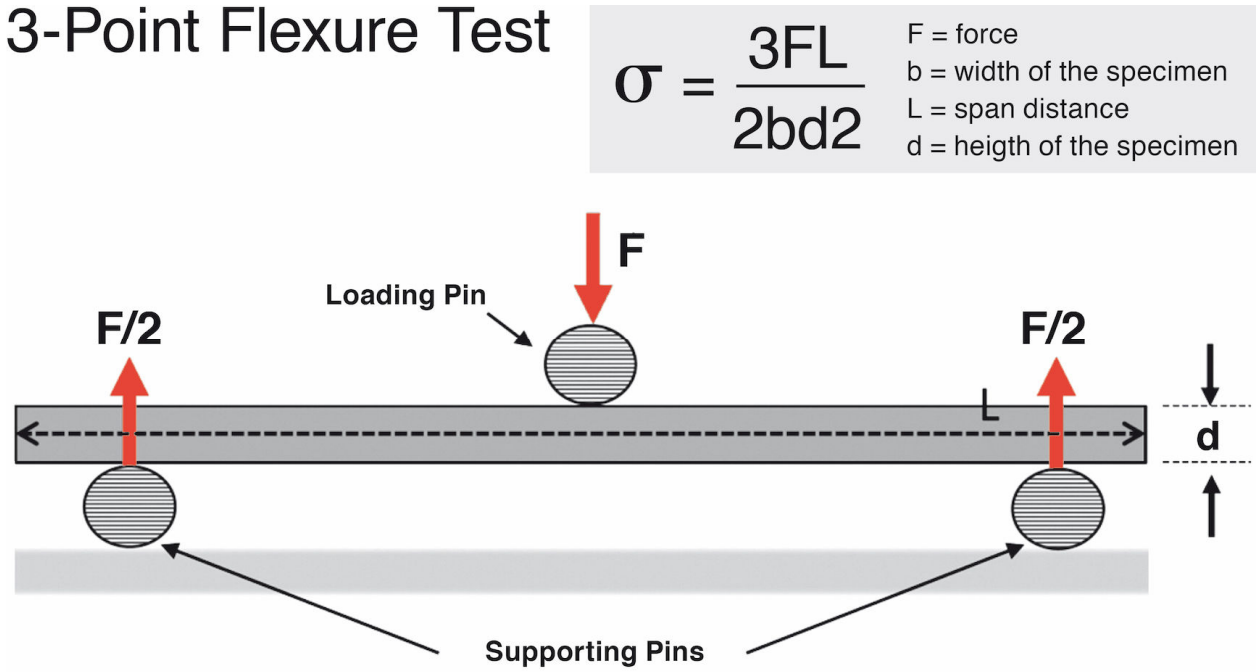

Figure 3. Schematic design of 3-point bending test.

2.4. Statistical Analysis

Shapiro–Wilk test was used to evaluate the normality of data. FS and Vickers microhardness values were analyzed using 1-way analysis of variance (ANOVA) and Bonferroni tests. All statistical analyses were performed using statistical software (SPSS v22.0; IBM Corp, Armonk, NY, USA) at a significance level of $\alpha = 0.05$.

3. Results

Descriptive statistics of FS values are given in Table 1. According to 1-way ANOVA, the differences among the FS values of test groups were nonsignificant (df = 3, F = 0.622, $p = 0.605$).

Table 1. Mean ±standard deviation flexural strength and Vickers microhardness values.

	Flexural Strength (MPa)	Vickers Microhardness (HV)
No-coat	68.1 ± 18.6 [a]	31.2 ± 10 [a]
Coat-15 s	62.8 ± 17.1 [a]	40.9 ± 12.3 [a]
Coat-20 s	63.9 ± 14.7 [a]	33.1 ± 7.3 [a]
Coat-30 s	71.6 ± 14 [a]	57.9 ± 10.4 [b]

Different superscript letters in columns show significant differences ($p < 0.05$).

The descriptive statistics for Vickers hardness values are given in Table 1. There were significant differences in hardness among test groups (df = 3, F = 14.326, $p < 0.001$). Coat-30 s had the highest microhardness values ($p \leq 0.003$). However, no significant differences in Vickers hardness values were observed among the remaining test groups ($p \geq 0.166$).

The surfaces of the specimens were rough and compact before thermocycling, while cracks and deteriorated surfaces were visible after thermocycling (Figure 4). Grains of SnO_2 and plates of graphene were clearly visible in the before-thermocycling FESEM images of Coat-15 s, Coat-20 s, and Coat-30 s that cannot be seen in the images of the No-coat group. Granules and voids were noticeable in the before-thermocycling FESEM images of No-coat

along with a rough surface for each group, which could be associated with the fact that no polishing was performed. When after-thermocycling FESEM images were evaluated, lines that indicate separation within graphene plates were visible in Coat-15 s, Coat-20 s, and Coat-30 s, while the granules had accumulated into plates with voids between them in No-coat (Figure 5). The Raman shift spectra of each group, which show the G-peaks of graphene for coated groups, are given in Figure 6. G-peaks are relatively short in comparison with the other peaks related to the tested PMMA.

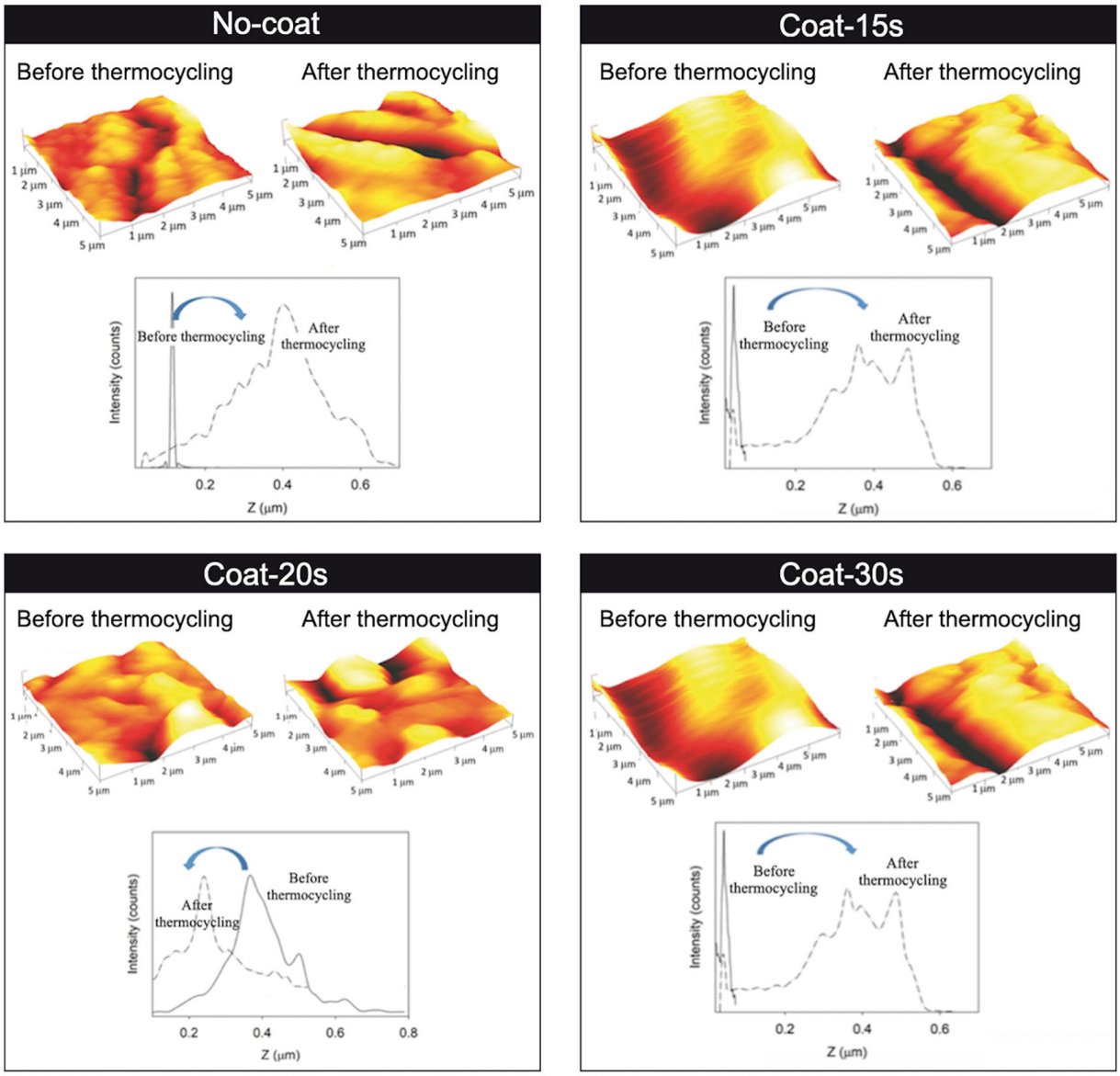

Figure 4. Representative atomic force microscopy images of each group before and after thermocycling.

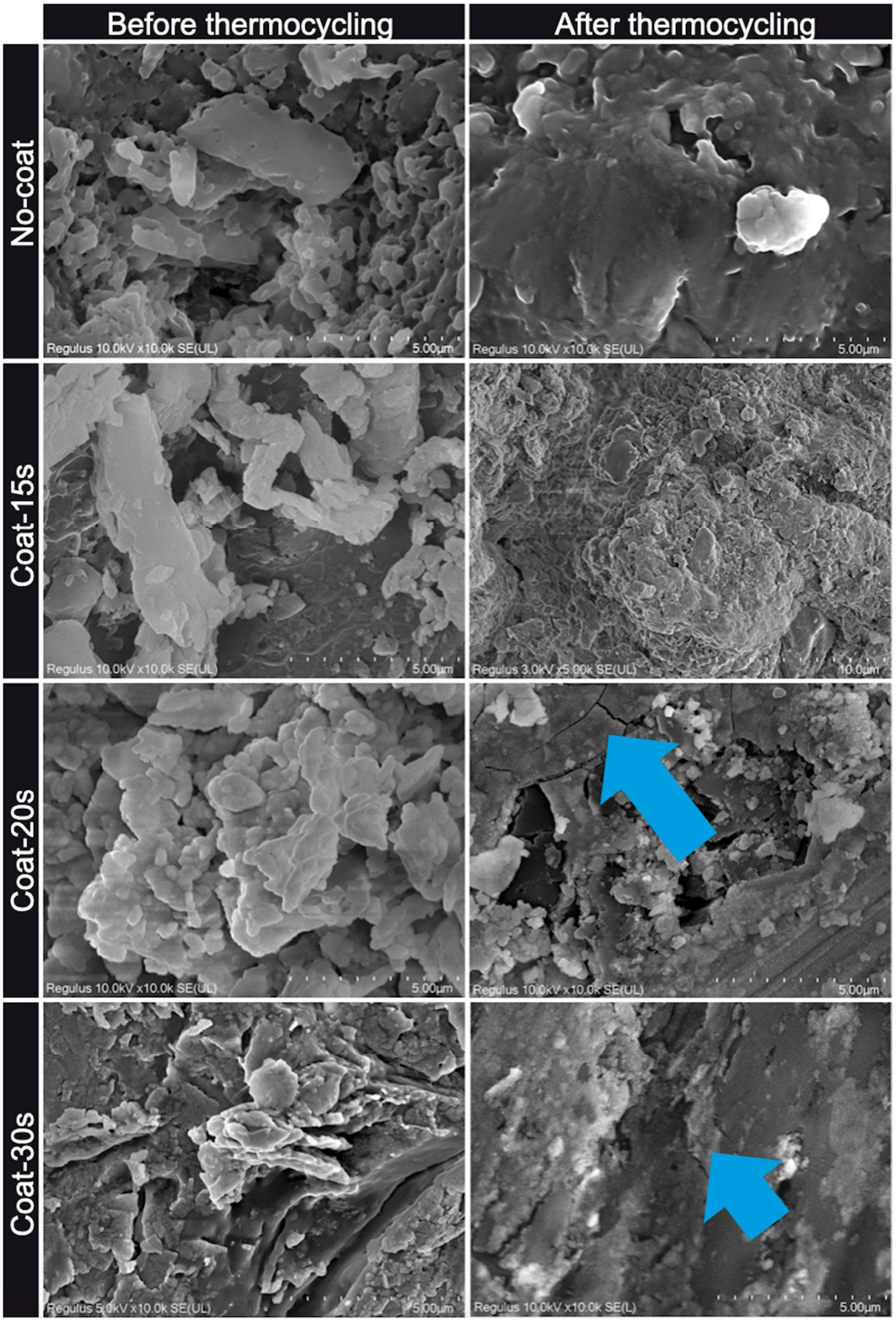

Figure 5. Representative FESEM images (×10,000) of one sample from each group before and after thermocycling. (Blue arrows indicate the cracks on surface coating after thermocycling.)

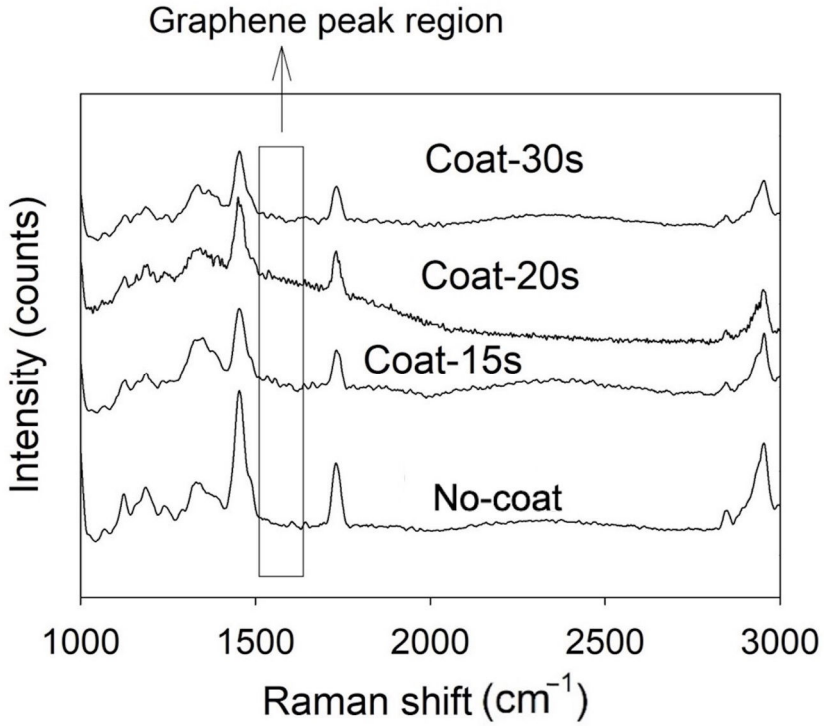

Figure 6. Representative Raman shift spectra of each group.

4. Discussion

The duration of the TVA process did not significantly affect the FS of the tested denture base resin. Therefore, the first hypothesis was rejected. However, the second hypothesis was accepted, as coating duration affected the Vickers hardness and Coat-30 s had the highest Vickers hardness among the test groups.

A denture base material should have a minimum FS of 65 MPa for proper functioning without irreversible deformation [2]. Even though there was no significant difference among the test groups in terms of FS, No-coat and Coat-30 s had mean FS values that were higher and Coat-15 s and Coat-20 s had mean FS values that were lower than the reported threshold of 65 MPa. However, the authors think that Coat-20 s also had acceptable FS values, given that a difference of 0.1 MPa may be clinically negligible. Considering these findings, it may be speculated that TVA affects FS values, and SnO_2-graphene thin film coating by TVA should not last less than 20 s or even 30 s, when Vickers hardness values were also considered. FESEM images of the SnO_2-graphene-coated groups also support this hypothesis, as increased duration was shown to lead to increased number of SnO_2 grains and graphene plates. Nevertheless, this interpretation needs to be supported by future studies using different durations of the TVA process.

Differences in the Vickers hardness between test groups may be related to the distribution of SnO_2-graphene on specimens' surfaces. The FTIR graphs of all SnO_2-graphene-coated groups had a perceivable transmittance peak at 3400.18 cm^{-1}; however, the graph of Coat-30 s had a different trend than those of Coat-15 s and Coat-20 s after this peak (Figure 2). While Coat-15 s and Coat-20 s had a noticeable increase in transmittance after the peak at 3400.18 cm^{-1}, a plateau was formed in Coat-30 s, which suggests a more uniform coating with SnO_2-graphene [31]. This result can be interpreted as the SnO_2-graphene coating enhancing the resistance of the tested heat-polymerized PMMA to thermocycling, which appears to be dependent of the duration of the TVA process. A smoother surface with a lesser number of separation lines that are relatively superficial within graphene plates was also visible in the after-thermocycling FESEM image of Coat-30 s when compared with those of Coat-15 s and Coat-20 s (Figure 5).

The FSs of the tested specimens in the present study was considerably lower than those reported in previous studies on graphene-reinforced PMMA [12,14,15]. Two of those

previous studies [12,15] evaluated the FS of prepolymerized PMMA disks with and without nanographene reinforcement. The authors have concluded that nanographene-reinforced PMMA had significantly higher FS values, with a mean value ranging from 89.58 MPa [15] to 113.03 Mpa [12]. In another study on mechanical properties of subtractively manufactured, nanographene-reinforced PMMAs in two different shades, it was also shown that the mean FS values were 145.4 MPa and 151.3 MPa [14]. The industrial polymerization process of nanographene-reinforced PMMA disks [2] may be associated with the higher FS results reported in those studies [12,14] compared with those in the present study, as this standardized fabrication process possibly leads to an equal distribution of graphene throughout the disks rather than covering the most superficial layer, as observed in the present study. However, those studies on the Vickers hardness of nanographene-reinforced PMMA disks [14,15] have reported lower values than those in the present study, particularly compared to the groups with SnO_2-graphene coating. It should be noted that a direct comparison between the present study and those previous studies [14,15] might be misleading because the specimens tested in the present study were fabricated from a heat-polymerizing PMMA. Nevertheless, the SnO_2-graphene coating tends to alter surface characteristics such as hardness, as TVA is a surface coating method [18] and graphene has strong chemical bonds between its own molecules that lead to high mechanical stability [14]. Di Carlo et al.'s [12] and Çakmak et al.'s [15] studies also support this hypothesis, as nanographene-reinforced PMMA disks were shown to have higher FSs than prepolymerized PMMA disks. The SnO_2-graphene coating of prepolymerized PMMA may be a cost-effective alternative to using reinforced PMMA disks, particularly when the duration and the ease of SnO_2-graphene coating process is considered. In addition, the prepolymerized PMMA disks can be costly and require the use of CAD-CAM tools, which are costlier than the equipment utilized to coat conventional heat-polymerized PMMA. However, a comparison between the mechanical properties of SnO_2-graphene-coated prepolymerized PMMA and nanographene-reinforced PMMA is needed to corroborate this hypothesis. Nevertheless, based on these interpretations, the SnO_2-graphene coating of nanographene-reinforced PMMA using TVA for at least 30 s may be an alternative combining the advantages of both reinforcement techniques. Future studies should investigate various PMMA modification possibilities.

In the present study, denture base resins were coated with SnO_2-graphene. Graphene was the essential component of the coating for the parameters tested in the present study due to its high mechanical stability along with its low cost [32]. However, the other component, SnO_2, which has already been tested in dental studies [22,33], has an antibacterial effect that may be particularly efficient considering that denture base materials are prone to deterioration and increased surface roughness due to intraoral stresses [15]. Because increased surface roughness might lead to denture stomatitis, one of the most commonly encountered complications for denture wearers [34], coating the denture bases with SnO_2-graphene using the TVS method may be a suitable alternative to increase the longevity of removable dentures, as graphene was also reported to have antibacterial activity [35]. Trends in the surface roughness of the tested groups also support this hypothesis, as the Coat-20 s and Coat-30 s samples had smoother surfaces after thermocycling than before thermocycling, whereas thermocycling led to rougher surfaces for the other groups (Figure 4). However, it should also be noted that Coat-20 s and Coat-30 s had rougher surfaces than other groups before thermocycling. Even though the average roughness of the specimens ranged between 40 nm and 160 nm in the present study, which is lower than the previously reported threshold of 0.2 µm for plaque accumulation [5], future in vivo studies on the surface roughness and bacterial plaque accumulation of SnO_2-graphene-coated denture base materials are needed to substantiate this hypothesis.

The fact that only one type of denture base resin was used in the present study is a limitation, and other denture base resins may lead to different results. In addition, only three time intervals for TVA were tested, and different application durations and other TVA settings may affect the results. Even though the surface topography of all groups was analyzed

using FESEM and AFM analyses, the structure of the SnO_2-graphene thin films was not evaluated using further analyses such as transmission electron microscopy. Thermocycling was performed using distilled water, and using a different medium, such as artificial saliva, may better simulate clinical conditions. In addition, no qualitative fractographic analysis was performed after the three-point bending test, and elaborating the fracture pattern of the specimens may broaden the effect of the SnO_2-graphene coating on heat-polymerized PMMA. Finally, even though FESEM and AFM images were used to qualitatively assess the surface topography of the specimens after thermocycling, the present study did not quantitatively analyze the effect of thermocycling on a SnO_2-graphene-coated denture base. Therefore, future studies should investigate different properties of SnO_2-graphene-coated denture base resins in different materials and the same properties using different tests with broadened TVA parameters to better comprehend the effect of this procedure on the properties of the materials it is applied on.

5. Conclusions

The graphene-doped SnO_2 coating of heat-polymerized PMMA using the tested thermionic vacuum arc method may be a suitable alternative to increase the longevity of removable dentures, as the surface roughness of the surfaces with this coating is low and graphene has been reported to have antibacterial activity.

Author Contributions: Conceptualization, C.A., E.M. and S.P.; Formal analysis, E.M.; Investigation, G.Ç., C.A. and S.P.; Methodology, C.A. and G.Ç.; Supervision, B.Y.; Writing—original draft, M.B.D., S.A.-A. and B.Y. All authors have read and agreed to the published version of the manuscript.

Funding: This research received no external funding.

Institutional Review Board Statement: Not applicable.

Informed Consent Statement: Not applicable.

Data Availability Statement: The data presented in this study are available on request from the corresponding author.

Conflicts of Interest: The authors declare no conflict of interest.

References

1. Aati, S.; Chauhan, A.; Shrestha, B.; Rajan, S.M.; Aati, H.; Fawzy, A. Development of 3D printed dental resin nanocomposite with graphene nanoplatelets enhanced mechanical properties and induced drug-free antimicrobial activity. *Dent. Mater.* **2022**, *38*, 1921–1933. [CrossRef] [PubMed]
2. Abualsaud, R.; Gad, M.M. Flexural strength of CAD/CAM denture base materials: Systematic review and meta-analysis of in-vitro studies. *J. Int. Soc. Prev. Community Dent.* **2022**, *12*, 160–170. [CrossRef] [PubMed]
3. Al-Dwairi, Z.N.; Tahboub, K.Y.; Baba, N.Z.; Goodacre, C.J.; Özcan, M. A comparison of the surface properties of CAD/CAM and conventional polymethylmethacrylate (PMMA). *J. Prosthodont.* **2019**, *28*, 452–457. [CrossRef]
4. Alp, G.; Johnston, W.M.; Yilmaz, B. Optical properties and surface roughness of prepolymerized poly(methyl methacrylate) denture base materials. *J. Prosthet. Dent.* **2019**, *121*, 347–352. [CrossRef] [PubMed]
5. Atalay, S.; Çakmak, G.; Fonseca, M.; Schimmel, M.; Yilmaz, B. Effect of thermocycling on the surface properties of CAD-CAM denture base materials after different surface treatments. *J. Mech. Behav. Biomed. Mater.* **2021**, *121*, 104646. [CrossRef]
6. Gruber, S.; Kamnoedboon, P.; Özcan, M.; Srinivasan, M. CAD/CAM complete denture resins: An in vitro evaluation of color stability. *J. Prosthodont.* **2021**, *30*, 430–439. [CrossRef]
7. Aldegheishem, A.; AlDeeb, M.; Al-Ahdal, K.; Helmi, M.; Alsagob, E.I. Influence of reinforcing agents on the mechanical properties of denture base resin: A systematic review. *Polymers* **2021**, *13*, 3083. [CrossRef]
8. Karci, M.; Demir, N.; Yazman, S. Evaluation of flexural strength of different denture base materials reinforced with different nanoparticles. *J. Prosthodont.* **2019**, *28*, 572–579. [CrossRef]
9. Gad, M.M.; Fouda, S.M.; Al-Harbi, F.A.; Näpänkangas, R.; Raustia, A. PMMA denture base material enhancement: A review of fiber, filler, and nanofiller addition. *Int. J. Nanomed.* **2017**, *12*, 3801–3812. [CrossRef]
10. Khosravani, M.R. Mechanical behavior of restorative dental composites under various loading conditions. *J. Mech. Behav. Biomed. Mater.* **2019**, *93*, 151–157. [CrossRef]
11. Aati, S.; Shrestha, B.; Fawzy, A. Cytotoxicity and antimicrobial efficiency of ZrO(2) nanoparticles reinforced 3D printed resins. *Dent. Mater.* **2022**, *38*, 1432–1442. [CrossRef]

12. Di Carlo, S.; De Angelis, F.; Brauner, E.; Pranno, N.; Tassi, G.; Senatore, M.; Bossù, M. Flexural strength and elastic modulus evaluation of structures made by conventional PMMA and PMMA reinforced with graphene. *Eur. Rev. Med. Pharmacol. Sci.* **2020**, *24*, 5201–5208.
13. Hernández, J.; Mora, K.; Boquete-Castro, A.; Kina, S. The effect of thermocycling on surface microhardness of PMMA doped with graphene: An experimental in vitro study. *J. Clin. Dent. Res.* **2020**, *17*, 152–161. [CrossRef]
14. Agarwalla, S.V.; Malhotra, R.; Rosa, V. Translucency, hardness and strength parameters of PMMA resin containing graphene-like material for CAD/CAM restorations. *J. Mech. Behav. Biomed. Mater.* **2019**, *100*, 103388. [CrossRef]
15. Çakmak, G.; Donmez, M.B.; Akay, C.; Abou-Ayash, S.; Schimmel, M.; Yilmaz, B. Effect of thermal cycling on the flexural strength and hardness of new-generation denture base materials. *J. Prosthodont.* **2023**, *32*, 81–86. [CrossRef]
16. Özgür, M.; Pat, S.; Mohammadigharehbagh, R.; Demirkol, U.; Akkurt, N.; Olkun, A.; Korkmaz, Ş. Two-dimensional BN-doped ZnO thin-film deposition by a thermionic vacuum arc system. *J. Mater. Sci. Mater. Electron.* **2020**, *31*, 6948–6955. [CrossRef]
17. Vladoiu, R.; Tichý, M.; Mandes, A.; Dinca, V.; Kudrna, P. Thermionic vacuum arc—A versatile technology for thin film deposition and its applications. *Coatings* **2020**, *10*, 211. [CrossRef]
18. Pat, S.; Korkmaz, Ş.; Balbağ, M.Z. A new deposition technique using reactive thermionic vacuum arc for ZnO thin film production. *J. Nanoelectron. Optoelectron.* **2014**, *9*, 437–441. [CrossRef]
19. Demirkol, U.; Pat, S.; Mohammadigharehbagh, R.; Musaoğlu, C.; Özgür, M.; Elmas, S.; Özen, S.; Korkmaz, Ş. Determination of the structural, morphological and optical properties of graphene doped SnO thin films deposited by using thermionic vacuum arc technique. *Phys. B Condens. Matter* **2019**, *569*, 14–19. [CrossRef]
20. Mohan, A.N.; Manoj, B. Surface modified graphene/SnO2 nanocomposite from carbon black as an efficient disinfectant against Pseudomonas aeruginosa. *Mater. Chem. Phys.* **2019**, *232*, 137–144. [CrossRef]
21. Munawar, T.; Nadeem, M.S.; Mukhtar, F.; Rehman, M.N.U.; Riaz, M.; Batool, S.; Hasan, M.; Iqbal, F. Transition metal-doped SnO(2) and graphene oxide (GO) supported nanocomposites as efficient photocatalysts and antibacterial agents. *Environ. Sci. Pollut. Res. Int.* **2022**, *29*, 90995–91016. [CrossRef] [PubMed]
22. Hsu, S.H.; Liao, H.T.; Chen, R.S.; Chiu, S.C.; Tsai, F.Y.; Lee, M.S.; Hu, C.Y.; Tseng, W.Y. The influence on surface characteristic and biocompatibility of nano-SnO(2)-modified titanium implant material using atomic layer deposition technique. *J. Formos. Med. Assoc.* **2022**, *122*, 230–238. [CrossRef] [PubMed]
23. Choudhary, A.K.; Gupta, A.; Kumar, S.; Kumar, P.; Singh, R.; Singh, P.; Kumar, V. Synthesis, antimicrobial activity, and photocatalytic performance of Ce doped SnO2 nanoparticles. *Front. Nanotechnol.* **2020**, *2*, 595352.
24. Khanom, R.; Parveen, S.; Hasan, M. Antimicrobial activity of SnO_2 nanoparticles against Escherichia coli and Staphylococcus aureus and conventional antibiotics. *Am. Sci. Res. J. Eng. Technol. Sci.* **2018**, *46*, 111–121.
25. Bacali, C.; Badea, M.; Moldovan, M.; Sarosi, C.; Nastase, V.; Baldea, I.; Chiorean, R.S.; Constantiniuc, M. The Influence of graphene in improvement of physico-mechanical properties in PMMA denture base resins. *Materials* **2019**, *12*, 2335. [CrossRef]
26. Bacali, C.; Baldea, I.; Moldovan, M.; Carpa, R.; Olteanu, D.E.; Filip, G.A.; Nastase, V.; Lascu, L.; Badea, M.; Constantiniuc, M.; et al. Flexural strength, biocompatibility, and antimicrobial activity of a polymethyl methacrylate denture resin enhanced with graphene and silver nanoparticles. *Clin. Oral Investig.* **2020**, *24*, 2713–2725. [CrossRef]
27. Lee, J.-H.; Jo, J.-K.; Kim, D.-A.; Patel, K.D.; Kim, H.-W.; Lee, H.-H. Nano-graphene oxide incorporated into PMMA resin to prevent microbial adhesion. *Dent. Mater.* **2018**, *34*, e63–e72. [CrossRef]
28. Simionescu, O.G.; Popa, R.C.; Avram, A.; Dinescu, G. Thin films of nanocrystalline graphene/graphite: An overview of synthesis and applications. *Plasma Process. Polym.* **2020**, *17*, 1900246. [CrossRef]
29. Gad, M.M.; Fouda, S.M.; Abualsaud, R.; Alshahrani, F.A.; Al-Thobity, A.M.; Khan, S.Q.; Akhtar, S.; Ateeq, I.S.; Helal, M.A.; Al-Harbi, F.A. Strength and surface properties of a 3D-printed denture base polymer. *J. Prosthodont.* **2022**, *31*, 412–418. [CrossRef]
30. *ISO 20795-1:2013*; Dentistry—Base polymers—Part 1: Denture Base Polymers. International Organization for Standardization (ISO): Geneva, Switzerland, 2013.
31. Querido, W.; Kandel, S.; Pleshko, N. Applications of vibrational spectroscopy for analysis of connective tissues. *Molecules* **2021**, *26*, 922. [CrossRef]
32. Al-Noaman, A.; Rawlinson, S.C.F. A novel bioactive glass/graphene oxide composite coating for a polyether ether ketone-based dental implant. *Eur. J. Oral Sci.* **2023**, *131*, e12915. [CrossRef]
33. Mumcu, E.; Topcu Ersöz, M.B.; Avukat, E.N.; Akay, C.; Pat, S. Influence of oxygen effect in coating layer on tensile bond strength of PMMA. *Int. J. Polym. Mater.* **2023**, *72*, 507–516. [CrossRef]
34. Stalder, A.; Berger, C.H.; Buser, R.; Wittneben, J.; Schimmel, M.; Abou-Ayash, S. Biological and technical complications in root cap-retained overdentures after 3-15 years in situ: A retrospective clinical study. *Clin. Oral Investig.* **2021**, *25*, 2325–2333. [CrossRef]
35. Lee, W.C.; Lim, C.H.Y.; Shi, H.; Tang, L.A.; Wang, Y.; Lim, C.T.; Loh, K.P. Origin of enhanced stem cell growth and differentiation on graphene and graphene oxide. *ACS Nano* **2011**, *5*, 7334–7341. [CrossRef]